

Analyst

Accepted Manuscript



This is an *Accepted Manuscript*, which has been through the Royal Society of Chemistry peer review process and has been accepted for publication.

Accepted Manuscripts are published online shortly after acceptance, before technical editing, formatting and proof reading. Using this free service, authors can make their results available to the community, in citable form, before we publish the edited article. We will replace this *Accepted Manuscript* with the edited and formatted *Advance Article* as soon as it is available.

You can find more information about *Accepted Manuscripts* in the [Information for Authors](#).

Please note that technical editing may introduce minor changes to the text and/or graphics, which may alter content. The journal's standard [Terms & Conditions](#) and the [Ethical guidelines](#) still apply. In no event shall the Royal Society of Chemistry be held responsible for any errors or omissions in this *Accepted Manuscript* or any consequences arising from the use of any information it contains.

In Situ Nanoparticle Sizing with Zeptomole Sensitivity

Christopher Batchelor-McAuley,^a Joanna Ellison^a, Kristina Tschulik^a, Philip L. Hurst^a, Regine Boldt^b, Richard G. Compton^{a}*

^aDepartment of Chemistry, Physical and Theoretical Chemistry Laboratory, University of Oxford, South Parks Road, Oxford OX1 3QZ, United Kingdom

^bLeibniz-Institut für Polymerforschung Dresden e.V. Hohe Str. 6, 01069 Dresden, Germany

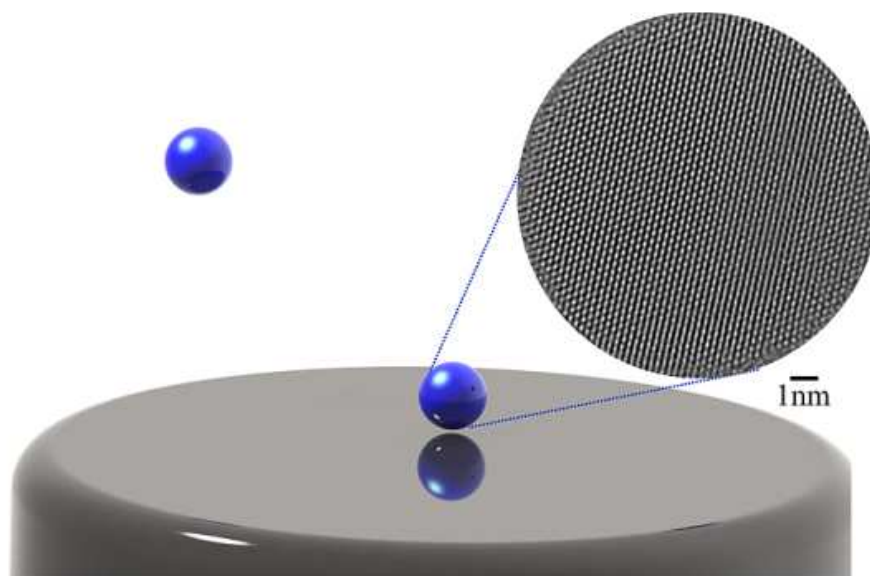
*Corresponding author. Fax: +44(0) 1865 275957
Email address: richard.compton@chem.ox.ac.uk

KEYWORDS

Nano-technology, Silver nanoparticles, Anodic particle coulometry, Brownian motion, carbon fibre electrodes

ABSTRACT

We present the basis for an entirely new approach to *in-situ nanoparticle sizing*. Nanoparticles containing just 12 zeptomoles (1 zeptomole = 10^{-21} moles) of silver, are detected *via in situ* particle coulometry. These stochastic charge measurements correspond to the transfer of only 7000-8000 electrons, yielding direct information relating to the individual nanoparticle volumes. The resulting particle size distribution (average equivalent radius 5 nm) obtained *via* nanoparticle coulometry is in excellent correspondence with that attained from TEM analysis. Moreover, the measurable particle size limit by this electrochemical method is shown to be significantly below that of more common optical nanoparticle tracking techniques, and as such can be viewed as a potential disruptive nano-technology.



INTRODUCTION

Individual nanoparticles can be detected by their direct redox response at an electrochemical interface.¹⁻⁵ A nanoparticle suspended in solution may randomly collide with an electrified surface resulting in small Faradaic bursts of charge. For an electrochemical system, the minimum measurable current is determined by the magnitude of the recorded noise.^{6, 7} These thermal fluctuations associated with the electrochemical interface cannot be considered solely in isolation of the measurement system. Hence, attainment of stochastic small particle detection by direct electrolysis of individual nanoparticles requires careful design of the experimental setup to ensure low-noise conditions.

As an alternative and well established approach the detection and localisation of individual particles (in non-opaque media) is possible by optical techniques.⁸⁻¹⁰ The detection of the light scattered from a particle with sub-wavelength dimensions allows the 2D and in certain circumstances the 3D^{11, 12} tracking of an individual particle position as a function of time. Consequently, *via* use of the Stokes-Einstein equation¹³ an *in-direct* measurement of the particle hydrodynamic radius is provided. Such technology forms the basis of commercial particle size analysers such as the 'Nanosight'⁸. However, an inherent limitation of the technique is the decrease in the scattered light intensity as a function of particle radius (Rayleigh scattering cross section $\propto r^6$).¹⁴ Even for strongly scattering plasmonic particles under optimal (i.e. non-optically opaque samples with dark-field illumination) conditions the inherent limit of detection is of particles of 10 - 20 nm in radius.¹⁵⁻¹⁷ Consequently, characterization of particles below this size limit must either be performed on a large ensemble (cf. dynamic light scattering¹⁸) or necessitates the study of the materials *ex-situ* by non-optical techniques such as scanning or transmission electron microscopy¹⁹.

Historically, the electrolytic sizing of electrochemically active particles found significant use in the chemical photographic industry from the early seventies²⁰ until the fields' subsequent demise with the advent of digital alternatives. Using a device which may be viewed as a forerunner of the electrochemical scanning microscope, the 'electrolytic grain size analyser', comprised of a metallic wire held at a relatively reducing potential. Through the use of a turntable, surface immobilised silver halide grains were mechanically brought into contact with the electrode. Upon contact the silver halide was reduced to silver and the resulting charge was recorded and related, *via* Faraday's first law, to the number of moles of silver halide contained within the particle, hence providing rapid and accurate sizing information.^{21, 22} The lower size limits for such particle

1
2
3 detection methods (0.1 - 0.2 μm diameter, corresponding to pico-coulombs of charge) was inherently limited
4
5 by the noise which predominantly resulted from the mechanical movement of the electrode. In 2011 a semi-
6
7 analogous technique of stochastic (nano) particle detection was developed.¹ For this modern technique the
8
9 particles of study are not surface supported but present in the solution phase and by virtue of Brownian
10
11 motion randomly come into contact with the electrode. With the particles being based in the solution phase
12
13 sample preparation is greatly simplified. More importantly, the problem of mechanical noise is overcome and
14
15 the detection of nanometer sized particles is enabled.
16
17

18
19 The work in this paper evaluates and evidences the practical limits of detection of small nanoparticles, using
20
21 in-situ particle coulometry. The magnitude of the electrolytic charge passed per nanoparticle is directly related
22
23 to the number of atoms contained in the particles, and thus the nanoparticle density and volume ($C \propto r^3$).
24
25 Hence, decreasing the measurable radius by a factor of two requires almost an order of magnitude
26
27 improvement of the signal-to-noise ratio of the system. However, through the careful design of the
28
29 electrochemical system in terms of the controlling and measurement circuits and the production of low
30
31 electrochemical-noise carbon fibre electrodes the measurement of femto-coulombs of charge is enabled,
32
33 resulting in the detection and quantification of nanoparticles as small as 3 nm in radius. These measurements
34
35 correspond to the passage of only a few- to tens-of-thousands (zeptomoles) of electrons occurring from
36
37 individual impact events. Importantly, this lower limit of detection is well below that available for common
38
39 stochastic optical scattering techniques (cf. 10 - 20 nm radius for plasmonic materials). Moreover, this
40
41 electrochemical technique is applicable to a wide range of substances including organic^{2, 23} metal oxide⁵ and
42
43 carbon²⁴ nanomaterials. As such the work provides a basis for a new disruptive nano-technology for particle
44
45 sizing.
46
47
48
49
50

51 **RESULTS AND DISCUSSION**

52
53 The following section is divided into three parts, first, the design requirements and parameterisation of the
54
55 noise response of the potentiostat system is discussed. Second, the detection and sizing of 5 nm radius silver
56
57 particles is evidenced and contrasted with other available techniques. Finally, the frequency of the
58
59
60

nanoparticle impacts is discussed evidencing the significant role of absorbed organics for nanoparticle electrolytic detection²⁵.

Design and characterisation of the potentiostat system:

The electrochemical instrumentation required for nanoparticle impact detection shares many of the specification requirements found with patch-clamp systems,²⁶ however two major differences arise. First, full potentiostatic control of the working (sense) electrode is highly desirable. Study of nanoparticle impacts as a function of potential yields both kinetic²⁷ and thermodynamic information and importantly provides a route by which the nanoparticles chemical composition may be probed⁴. Control of the working electrode potential in a low noise system is best achieved through the use of a highly stabilised three-electrode potentiostat circuit. Second, due to the possibility of the occurrence of deleterious electrochemical side reactions it is preferential that the electrochemical cell can be readily disconnected between experiments. In the present work, this feature is achieved by the incorporation of a computer controlled relay switch on the counter (auxiliary) electrode. Disconnection of the counter electrode electrically isolates the working electrode ensuring no charge is passed between experiments.

Next the work briefly considers the theoretical noise response of the electrochemical system. The limitation of any electrical current measurement arises from thermal noise.²⁸ For a resistor the distribution of the noise current as a function frequency S (A^2/Hz) is⁷,

$$S = 4k_B T/R \quad \text{Equation 1}$$

where k_B is the Boltzmann constant ($1.38 \times 10^{-23} \text{ J K}^{-1}$), T is the temperature (K) and R is the magnitude of the resistor (Ω). Integration of power spectral density (Equation 1) with respect to frequency yields the variance (σ_{rms}^2) of the thermal noise over the bandwidth of interest. As it is not energy dispersive an ideal capacitor is not a source of thermal noise. However, the behaviour of a capacitor in series with a voltage noise source is an important consideration. Here the frequency dependent noise current power spectral density is given by,²⁶

$$S = (2\pi f C_{\text{tot}})^2 S_v \quad \text{Equation 2}$$

where f is the bandwidth of the measurement, C_{tot} is the total capacitive load and S_v is the source noise voltage.

For an electrochemical system where the current is measured using a transimpedance amplifier (current-to-voltage converter), the dominant thermal noise may originate from either the electrochemical cell or the amplifier²⁹. First, for the current-to-voltage converter the magnitude of the feedback resistor serves to determine both the amplifiers gain and the minimum noise. For example for a 1 gigaohm feedback resistor gives a gain (I/V) of 10^9 and in accordance with Equation 1 the power spectral density of the noise current is theoretically predicted to be $1.6 \times 10^{-29} \text{ A}^2/\text{Hz}$. This value gives the minimum possible noise originating from the system. The noise response of the electrochemical interface is more complex², however at higher frequencies and for larger electrodes the capacitive loading of the amplifier by the electrode leads to a response in accordance with Equation 2. For the current-amplifier used in this work the noise voltage is reported to be 5nV/Hz at 1kHz.

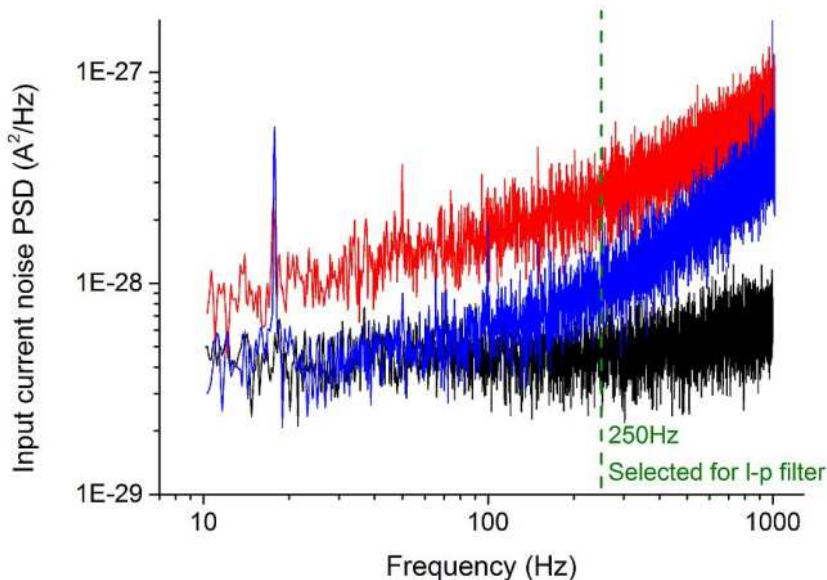


Figure 1: Input-referred current (folded) power spectral density; black is the potentiostat 'noise floor', blue is a carbon fibre coated in polymer, and red is a commercial glass sealed carbon fibre.

Figure 1 depicts the input-referred current power spectral density of the proposed electrochemical system. Measurement of the potentiostat noise floor was achieved with the working electrode disconnected and in the absence of the 4-pole Bessel filter used in the later experiments. The 'noise floor' for the system is measured

1
2
3 to be $\sim 4 \times 10^{-29} \text{ A}^2/\text{Hz}$ (10-500 Hz) and only marginally above the theoretically predicted value of $1.6 \times 10^{-29} \text{ A}^2/\text{Hz}$
4
5 (Equation 1, with a 1 G Ω feedback resistor). It should be noted that the power spectral response of a high-
6
7 quality commercially available potentiostat yields a noise response that is between one to two orders of
8
9 magnitude larger (see SI section 1). Also depicted in Figure 1 are the power spectral densities with the
10
11 connection of a commercial glass sealed carbon fibre electrode and the polymer coated carbon fibre
12
13 (fabrication described in the experimental). Importantly, the noise response of the polymer coated electrode is
14
15 below that of the glass sealed electrode. This decrease in the noise response likely reflects the different
16
17 electrode surface preparation procedures. Despite having the same geometric surface areas, (both carbon
18
19 fibres are 7 μm in diameter) it is concluded that the polishing surface preparation method used for the
20
21 commercial carbon fibre results in an enhanced surface roughness, thus leading to a higher electroactive
22
23 surface. Conversely, the cut carbon fibre exhibits a smaller electroactive surface area.³⁰ This conclusion is
24
25 corroborated by comparison of the cyclic voltammetric responses of the two electrodes with the glass sealed
26
27 electrode showing a significantly larger capacitive current (SI, section 3), noting that the capacitance is
28
29 proportional to the electroactive area. For the polymer coated carbon fibre the noise response up to
30
31 approximately 100 Hz is limited by the current-amplifier, above this frequency the noise response increases
32
33 and reflects the capacitive loading of the amplifier as predicted by Equation 2. Consequently, due to the larger
34
35 noise response at higher frequencies the system was filtered to 250 Hz using an active low-pass 4-pole Bessel
36
37 filter. From the averaging of 6 separate recordings of the systems noise of the polymer coated carbon fibre
38
39 electrodes filtered to 250Hz, the root-mean-square noise (σ_{rms}) was found to maximally be 0.23pA. Finally, the
40
41 PSD response of the 250Hz Bessel filter is depicted in the SI section 1.
42
43
44
45
46
47
48
49
50
51
52
53
54
55
56
57
58
59
60

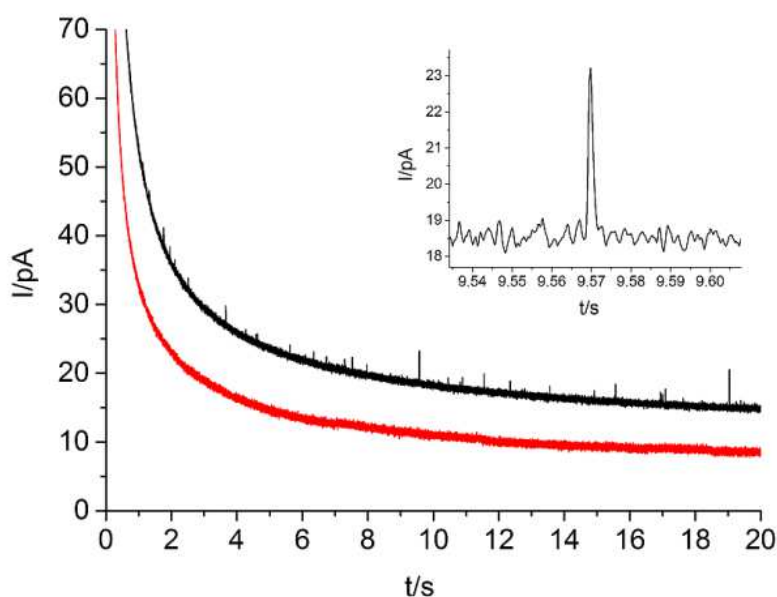


Figure 2: Chronoamperograms of the coated wire micro-electrode in the presence of 20 mM trisodium citrate. The red line shows a scan in the absence of nanoparticles and the black line demonstrates faradaic spikes in the presence of 38 pM AgNPs.

Silver nanoparticle detection:

To demonstrate the lower size limit for nanoparticle detection nano-impact experiments were performed on the low noise potentiostat system described above using the synthesised citrate capped AgNPs. For this a solution of 20 mM trisodium citrate was used as supporting electrolyte in order to minimise AgNP aggregation/agglomeration. Pre-dispersed AgNPs were added to give a final nanoparticle concentration of 38 pM in the solution. Chronoamperograms were run for a time of 20 seconds each, applying a potential of 0.6 V vs MSE reference electrode; a potential positive enough as to allow complete oxidation of the impacting AgNPs³¹.

Initially chronoamperograms were run in a blank citrate solution containing no AgNPs. In this system no nanoparticle impact spikes were observed during the chronoamperograms. On addition of the nanoparticles to this solution faradaic spikes are observed and can be seen in Figure 2 demonstrating that any oxidative spikes seen were due to the presence of AgNPs in the solution and their subsequent oxidation. The observed spikes were included in analysis if their spike height was determined to be a minimum of three times the root mean square noise, giving a total of 290 nanoparticle impact spikes to be counted. Integration of the area under

each of these impact spikes gives a value for the charge passed per nanoparticle and a distribution of the charges is obtained (see SI section 2). The lowest charge measured was 1.22 fC ($1 \text{ fC} = 10^{-15} \text{ C}$) corresponding to the oxidation of just 7,620 silver atoms.

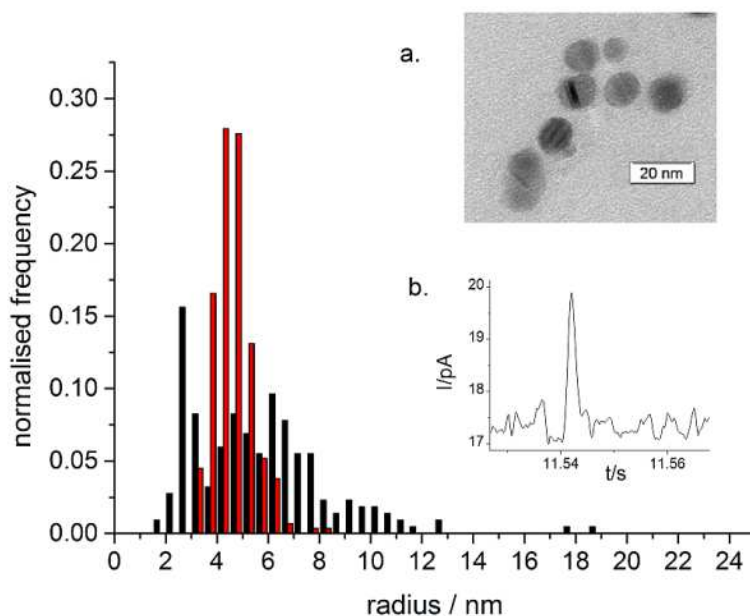


Figure 3: A histogram showing the size distribution for AgNPs as determined by impact experiments (red) and TEM analysis (black). Inlay a) shows an example TEM image of the nanoparticles, and inlay b) shows an example impact spike.

The charge passed per impact spike can be directly related to the number of moles of silver in the nanoparticle by application of Faraday's Law. This can be converted, assuming the particles to be spherical, to a value for the nanoparticle radius and hence provides a measure of the size of the impacting nanoparticles⁴. A histogram of the nanoparticle radius distribution was obtained and is shown in Figure 3. The mean AgNP radius was determined to be 4.7 nm with a standard deviation of 0.8 nm. Additional nanoparticle sizing performed using DLS and TEM analysis. DLS analysis shows a nanoparticle size distribution in the same region as nanoparticle impact data (See SI section 4). However, it should be noted that DLS is heavily weighted towards larger nanoparticles due to the r^6 dependency of Rayleigh scattering. Moreover, DLS gives a measure of the hydrodynamic radius of the nanoparticle and thus values for nanoparticle radius will be larger than those obtained *via* TEM or impact experiments. TEM analysis further corroborates the impact data, giving a nanoparticle radius of $5.7 \pm 2.7 \text{ nm}$ in good agreement with the nanoparticle impact sizing data (further TEM images can be found in SI section 4). The standard deviation of the TEM analysis is found to be larger than that determined by the nanoparticle impact experiments. This artefact can be attributed to the asymmetry of the

1
2
3 nanoparticles. If a nanoparticle is even slightly oblate in shape, then the perceived size, and thus radius, will
4 depend on the angle at which it was viewed during the TEM measurements, effectively leading to a
5 broadening of the size distribution. Conversely, for nanoparticle impact experiments the measured parameter
6 is charge. As the charge is related to the number of atoms in the nanoparticle, it is dependent on the total
7 nanoparticle *volume* and is independent of shape. Hence, an impacting spherical or an oblate nanoparticle of
8 the same total volume will give the same result, thus leading to a smaller standard deviation. Nevertheless, it
9 can be seen that nanoparticle impact experiments are in close agreement with the results and provide an
10 accurate method for the *in situ* sizing of small AgNPs. Indeed AgNPs with a radius as low as 3.1 nm (7000-8000
11 electrons) were detected, characterised and sized by the nanoparticle impact method.
12
13
14
15
16
17
18
19
20
21
22
23
24

25 Frequency of the nanoparticle impacts:

26
27
28 The use of the coated wire electrodes allows for the quick and easy regeneration of a fresh, clean electrode
29 surface during the impact experiment. It has previously been demonstrated that nanoparticle impact
30 experiments are highly sensitive to electrode surface fouling effects²⁵. The adsorption of organic molecules to
31 the electrode surface blocks off areas of the surface and prevents the nanoparticle approaching close enough
32 to make electrical contact with the electrode. Thus, the number of nanoparticles that are able to be oxidised is
33 reduced. Prolonged exposure to the electrolyte solution allows fouling molecules to become adsorbed and
34 hence reduces the efficiency of the impact experiment. By simply re-slicing off the end of the coated wire
35 electrodes a fresh micro-electrode surface is generated, allowing the blocking effect to be minimised and
36 nanoparticle impacts to be restored. The effect of this surface fouling and subsequent regeneration can be
37 seen in Figure 4. Here, 20 - 30 nanoparticle impacts are observed during the 20 second chronoamperogram
38 after a freshly sliced electrode has initially been submerged into the electrolyte. However, as the number of
39 scans recorded increases and thus the amount of time the electrode has been in the solution rises, the number
40 of impacts per scan can be seen to decrease. This decrease is observed for successive scans and the number of
41 impacts observed rapidly falls to zero. Slicing off the electrode tip provides a clean surface, and is reflected by
42 a sharp increase in the total number of nanoparticle impacts. These then decreases back down to zero as
43 surface fouling begins to dominate again.
44
45
46
47
48
49
50
51
52
53
54
55
56
57
58
59
60

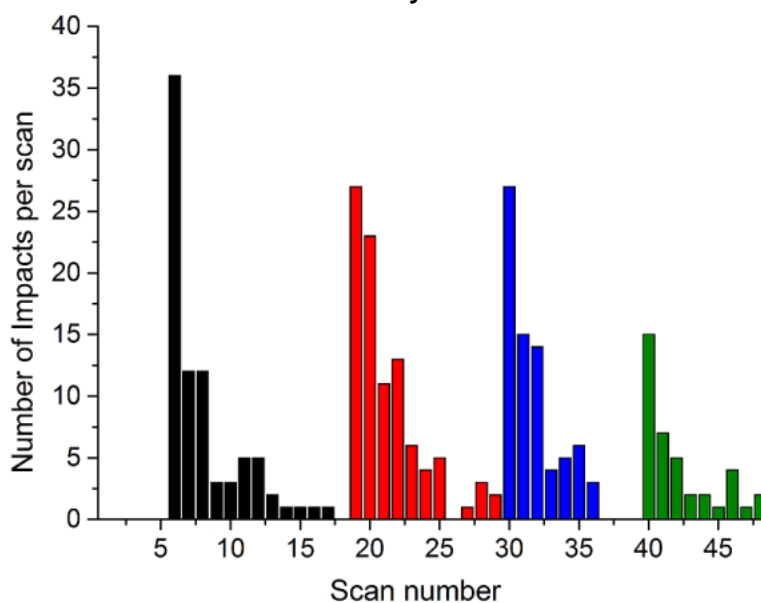


Figure 4: The total number of nanoparticle impacts observed per scan after addition of 38 pM silver nanoparticles at Scan 0. The electrode is 'activated' by renewing the surface after scan five, clearly demonstrating the influence of adsorbed molecular species on the electrode surface; Black following the initial electrode re-slicing, red following the second re-slicing, blue the third and green the fourth electrode re-slicing.

After the nanoparticles were initially added to the electrolyte system no nanoparticle impacts were observed during the first five scans. At this stage the electrode had been pre-exposed to the electrolyte solutions. This therefore evidences the fact that electrode fouling is due to electrolyte exposure and subsequent sticking of adsorbing species as opposed to an effect of the nanoparticle impacts themselves or the aging of the nanoparticles in the electrolyte. Once the electrode was recut in the presence of nanoparticles, impacts were seen immediately. Importantly, when an electrode was placed in a citrate solution in the absence of nanoparticles after it had been re-sliced no impact spikes were observed for multiple times of re-slicing.

It should be noted that although this method for providing a refreshed electrode surface provides a significant enhancement to the number of nanoparticle impacts, the theoretical number of impacts predicted for the nanoparticle concentration used is not obtained. A formula for the expected cumulative number of impacts per scan (assuming a Fickian model) has previously been estimated by integration of the Szabo equation by series expansion⁴. At the 38 pM concentration of AgNPs used in this work the predicted number of impacts in 20 seconds is 375. However, at this concentration (38 pM) the separation between nanoparticles becomes larger than the diffusion layer thickness at the electrode, and therefore Fickian statistics break down. Consequently, the predicted number of nanoparticle impacts is an approximation.

CONCLUSIONS

The lower size limit for nanoparticle detection by nanoparticle coulometry has been established and demonstrated experimentally. It has been shown that silver nanoparticles with a mean radius of 4.7 nm are able to be detected and sized electrochemically, and indeed particles as small as 3.15 nm in radius were characterised and the sizing data is in excellent correspondence with TEM results. This nanoparticle detection limit is achievable due to the minimisation of the electrical noise of the system by the design of the potentiostat and use of low noise carbon fibre micro-electrodes. These values are significantly lower than those currently obtainable by optical techniques, and thus we have shown the importance of electrochemical particle coulometry as a means of detecting and characterising small nanoparticles in a solution media. While the study presented herein focusses on the sizing of ultra-small Ag nanoparticles, the analytical method of particle coulometry in conjunction with the newly developed potentiostat and carbon fibre micro-electrodes may conveniently be used to decrease the minimum detectable particle size of other nanoparticles, such as metal (e.g. Au^3 , Ni^4), metal oxide (Fe_3O_4^5), carbonaceous (C_{60}^{24}) or organic (indigo²) nanoparticles.

METHODS

Electrochemical apparatus:

A three electrode cell was used comprising of a carbon fibre working electrode (fabrication described below), a mercury sulphate reference electrode (MSE = +0.65V vs NHE, BASi Inc.) and a platinum mesh counter electrode (Goodfellow, Cambridge Ltd) completing the circuit. Potentiostatic control and measurement of the impact current transients were enabled by the use of the in-house built low noise potentiostat. This potentiostat comprises of three main sections; the computer interface used for analog-to-digital and digital-to-analog conversion, the current amplifier circuit and the highly stabilized potentiostat. A Labjack U6 (Labjack corporation, Lakewood, CO USA), with a Labjack tickDAC, was used for the computer interface. Connection to the Labjack was *via* a standard USB but with the ground isolated from that of the PC (USB-ISO OLIMEX, Farnell, Leeds, UK). Control of the Labjack was performed *via* a script written in Python 2.7 and run through the IDE Canopy (Enthought, Austin, TX USA). Measurement of the current at the working electrode (running to ground) was achieved with a low current-amplifier LCA-4K-1G (FEMTO, Messtechnik GmbH, Germany) and the bandwidth of the output of the current amplifier was limited using a 250 Hz 4-pole Bessel filter, Linear

1
2
3 Technology DC338A-B (Farnell, Leeds, UK). The resulting analogue signal was oversampled and digitized using
4
5 the Labjack at a stream rate of 4 kHz. Potentiostatic control was provided by a highly stabilized (1kHz
6
7 bandwidth) classic adder potentiostat³². Importantly, first, for the reference buffer a high quality operational-
8
9 amplifier with an ultra low-input bias (25 fA) was used, LMC6001 (Farnell, Leeds, UK). Second, a high quality
10
11 low-noise operational-amplifier, AD797 (Farnell, Leeds, UK), provided the control of the potential at the
12
13 counter electrode.
14

15
16 Measurement of the power spectral density (PSD):
17

18
19 For a general measurement of the PSD 60 seconds of noise data was recorded at 30 kHz in the absence of any
20
21 additional analog filter for a period of 60 seconds. This noise data was sub-divided into ten 6 second sections.
22
23 Using a script written in Python 2.7 the full power spectral density was calculated by means of a fast Fourier
24
25 transform. The resulting PSD was folded and subsequently averaged across the ten sets of noise data.
26
27
28
29
30
31
32
33

34 Electrode fabrication:

35
36 Carbon fibre wire electrodes were fabricated and insulated with a polymer coating, forming a micro-disc
37
38 electrode by slicing off the coated electrode tip. First, carbon fibre of diameter 7 μm (Goodfellow, Cambridge
39
40 Ltd) was attached to a conducting metal wire by silver epoxy conductive adhesive (RS Components Ltd.). The
41
42 adhesive was then heat set in an oven for 15 minutes at 150 °C. The electrodes were then insulated by the
43
44 formation of a phenol - allyl phenol copolymer based on a previously reported method³³. Here the carbon fibre
45
46 electrode was submerged into a freshly prepared 1:1 methanol to water solution containing 60 mM phenol, 90
47
48 mM 2-allyl phenol and 156 mM 2-butoxyethanol. A potential of 5 V was held between the carbon fibre
49
50 electrode and a platinum wire counter electrode for 40 minutes. The electrode was then removed from the
51
52 solution and placed in an oven at 150 °C for 30 minutes to allow the coating to cure. Next, the carbon fibre
53
54 electrode was sealed inside a plastic pipette tip using wax to seal the apex and prevent any leakage of
55
56 electrolyte solution onto the conducting metal wire during experiments. Finally, the tip of the coated carbon
57
58 fibre was sliced off using a razor blade to expose a micro-disc electrode.
59
60

1
2
3 To confirm that the electrodes were successfully covered by the polymer images of a bare carbon fibre and a
4 coated carbon fibre were imaged using SEM (Jeol JSM-6010LV) analysis. For this the carbon fibres were
5 immobilised on carbon tape and covered with a thin layer of evaporated gold to increase conductivity. The
6 images indicate that following the polymerisation the carbon fibre is covered in a thin, uniform polymer
7 insulation layer across the whole carbon fibre surface. Additionally, the electrodes were characterised by
8 running cyclic voltammograms in 1 mM hexamine ruthenium chloride and 0.1 M KCl and measuring the steady
9 state response. The values of the steady state current obtained indicated that the electrode was fully insulated
10 and that a micro-disc electrode was formed (see SI, section 3).
11
12
13
14
15
16
17
18
19

20
21 Silver nanoparticle synthesis:

22
23 Citrate-capped AgNPs were synthesised based on a method previously reported by Wan *et al.*³⁴. Briefly, a
24 solution of trisodium citrate in water was heated to 70 °C. Silver nitrate and sodium borohydride solutions
25 were then brought up to this temperature and were added to the citrate solution with constant stirring. The
26 solution was then left to stir at 70 °C for one hour before being cooled back down to room temperature. The
27 resulting product was a suspension of 5 nm AgNPs. The size of the nanoparticles was confirmed by TEM
28 analysis, UV-vis spectroscopy (Hitachi U-2001) and DLS (Zetasizer Nano ZS, Malvern) and results can be seen in
29 SI section 4. TEM investigations were performed using a Zeiss Libra 120MS with a LaB6-cathode equipped with
30 an Omega-Energy filter working at 120 KV. 5 µL of an aqueous suspension treated with ultrasound for 5
31 seconds was placed on a copper grid coated with a carbon hole film. To avoid agglomeration the supernatant
32 solution was removed by using filter paper after 10 seconds. The TEM images show spherical silver
33 nanoparticles with a mean radius of 5.7 ± 2.7 nm.
34
35
36
37
38
39
40
41
42
43
44
45
46

47 Reagents and Equipment:

48
49 All chemicals were purchased from Sigma Aldrich unless otherwise stated and all solutions were made using
50 ultrapure water, (Millipore, resistivity not less than 18.2 MΩ cm at 25 °C).
51
52
53
54

55 Before nanoparticle impact experiments all glassware was cleaned using aqua regia (3:1 hydrochloric acid:
56 nitric acid) for 30 minutes and subsequently sonicated in water for 15 minutes to remove any AgNP
57 contaminants that may have adsorbed to the glassware. The platinum mesh counter electrode was cleaned by
58 flame cleaning.
59
60

1
2
3 Electrochemical impact experiments were conducted in an aqueous solution of 20 mM trisodium citrate as the
4 electrolyte. Stock suspension of Ag NPs was added to this electrolyte to yield a concentration of 38 pM Ag NPs.
5
6 Chronoamperograms were recorded at a potential of 0.6 V vs MSE, which had previously been found to allow
7
8 quantitative sizing of Ag NPs in the used electrolyte^{31,35}.

9
10
11 Analysis of impact spikes was performed using SignalCounter, developed by Dario Omanovic^{36, 37}, (Centre for
12 Marine and Environmental Research, Ruder Boskovic Institute, Croatia). This allowed for determination of the
13 baseline, baseline correction, selection of impact spikes dependent on their magnitude, and finally
14 determination of the peak area of the spikes. Subsequent data analysis was performed in OriginPro 9 (Origin
15 Lab Corporation).

22 23 **SUPPORTING INFORMATION AVAILABLE**

24
25
26 The following are available in the supporting information: current power spectral density plots for different
27 potentiostat models, and for the used system with and without a filter; a histogram showing the charge
28 distribution obtained *via* nanoparticle impact experiments; cyclic voltammograms of a commercial and
29 fabricated electrode in 1.0 mM hexamine ruthenium chloride with 0.1 M KCl; SEM images of an uncoated
30 carbon fibre and a carbon fibre following the polymerisation procedure; and UV-Vis spectroscopy, TEM images
31 and DLS data of the synthesised silver nanoparticles.

38 39 40 41 42 **ACKNOWLEDGEMENTS**

43
44
45 The research leading to these results has received funding from the European Research Council under the
46 European Union's Seventh Framework Programme (FP/2007-2013) / ERC Grant Agreement n. [320403]. KT was
47 supported by a Marie Curie Intra European Fellowship within the 7th European Community Framework
48 Programme
49
50
51
52
53
54
55
56
57
58
59
60

REFERENCES

1. Zhou, Y.-G.; Rees, N. V.; Compton, R. G. The Electrochemical Detection and Characterization of Silver Nanoparticles in Aqueous Solution. *Angewandte Chemie International Edition* 2011, 50, 4219-4221.
2. Cheng, W.; Zhou, X.-F.; Compton, R. G. Electrochemical Sizing of Organic Nanoparticles. *Angewandte Chemie International Edition* 2013, 52, 12980-12982.
3. Zhou, Y.-G.; Rees, N. V.; Pillay, J.; Tshikhudo, R.; Vilakazi, S.; Compton, R. G. Gold Nanoparticles Show Electroactivity: Counting and Sorting Nanoparticles Upon Impact with Electrodes. *Chemical Communications* 2012, 48, 224-226.
4. Stuart, E. J. E.; Zhou, Y.-G.; Rees, N. V.; Compton, R. G. Determining Unknown Concentrations of Nanoparticles: The Particle-Impact Electrochemistry of Nickel and Silver. *RSC Advances* 2012, 2, 6879-6884.
5. Tschulik, K.; Haddou, B.; Omanović, D.; Rees, N.; Compton, R. Coulometric Sizing of Nanoparticles: Cathodic and Anodic Impact Experiments Open Two Independent Routes to Electrochemical Sizing of Fe₃O₄ Nanoparticles. *Nano Res.* 2013, 6, 836-841.
6. Carminati, M.; Vergani, M.; Ferrari, G.; Caranzi, L.; Caironi, M.; Sampietro, M. Accuracy and Resolution Limits in Quartz and Silicon Substrates with Microelectrodes for Electrochemical Biosensors. *Sensors and Actuators B: Chemical* 2012, 174, 168-175.
7. Yao, J.; Gillis, K. D. Quantification of Noise Sources for Amperometric Measurement of Quantal Exocytosis Using Microelectrodes. *Analyst* 2012, 137, 2674-2681.
8. Filipe, V.; Hawe, A.; Jiskoot, W. Critical Evaluation of Nanoparticle Tracking Analysis (NTA) by NanoSight for the Measurement of Nanoparticles and Protein Aggregates. *Pharm Res* 2010, 27, 796-810.
9. Lapresta-Fernández, A.; Salinas-Castillo, A.; Anderson de la Llana, S.; Costa-Fernández, J. M.; Domínguez-Meister, S.; Cecchini, R.; Capitán-Vallvey, L. F.; Moreno-Bondi, M. C.; Marco, M. P.; Sánchez-López, J. C.; Anderson, I. S. A General Perspective of the Characterization and Quantification of Nanoparticles: Imaging, Spectroscopic, and Separation Techniques. *Critical Reviews in Solid State and Materials Sciences* 2014, 39, 423-458.
10. Zhu, S.; Wang, S.; Yang, L.; Huang, T.; Yan, X. Progress in the Development of Techniques Based on Light Scattering for Single Nanoparticle Detection. *Sci. China Chem.* 2011, 54, 1244-1253.
11. Batchelor-McAuley, C.; Martinez-Marrades, A.; Tschulik, K.; Patel, A. N.; Combellas, C.; Kanoufi, F.; Tessier, G.; Compton, R. G. Simultaneous Electrochemical and 3D Optical Imaging of Silver Nanoparticle Oxidation. *Chemical Physics Letters* 2014, 597, 20-25.
12. Martinez-Marrades, A.; Rupprecht, J.-F.; Gross, M.; Tessier, G. Stochastic 3D Optical Mapping by Holographic Localization of Brownian Scatterers. *Opt. Express* 2014, 22, 29191-29203.
13. Einstein, A. *Annalen der Physik* 1905, 322, 549-560.
14. Moosmüller, H.; Arnott, W. P. Particle Optics in the Rayleigh Regime. *Journal of the Air & Waste Management Association (1995)* 2009, 59, 1028-1031.
15. Boyer, D.; Tamarat, P.; Maali, A.; Lounis, B.; Orrit, M. Photothermal Imaging of Nanometer-Sized Metal Particles Among Scatterers. *Science* 2002, 297, 1160-1163.
16. Crut, A.; Maioli, P.; Del Fatti, N.; Vallee, F. Optical Absorption and Scattering Spectroscopies of Single Nano-Objects. *Chemical Society Reviews* 2014, 43, 3921-3956.
17. *Measurements relying on the Rayleigh scattering, such as dark field microscopy are limited to nanoparticle detection of particles ~ 10 - 20 nm in radius. Smaller nanoparticles, down to 2.5 nm can be in directly detected by photothermal imaging where a laser pulse induces a temperature rise local to the nanoparticle. See ref. 17.*
18. Pecora, R. Dynamic Light Scattering Measurement of Nanometer Particles in Liquids. *Journal of Nanoparticle Research* 2000, 2, 123-131.

19. Ponce, A.; Mejía-Rosales, S.; José-Yacamán, M. Scanning Transmission Electron Microscopy Methods for the Analysis of Nanoparticles. In *Nanoparticles in Biology and Medicine*, Soloviev, M., Ed. Humana Press: 2012; Vol. 906, pp 453-471.
20. Moller, G. Grain Size Determination of Silver Halide Crystallites by Electrochemical Reduction. *Chimia* 1971, 25, 29.
21. Holland, A. B.; Feinerman, A. D. An Improved Electrolytic Grain-Size Analyzer. *Journal of Applied Photographic Engineering* 1982, 8, 165-167.
22. Holland, A. B.; Sawers, J. R. Grain Size Determination by Electrolyte Reduction. *Photographic Science and Engineering* 1973, 17, 295-298.
23. Cheng, W.; Compton, R. G. Investigation of Single-Drug-Encapsulating Liposomes using the Nano-Impact Method. *Angewandte Chemie International Edition* 2014, n/a-n/a.
24. Stuart, E. J. E.; Tschulik, K.; Batchelor-McAuley, C.; Compton, R. G. Electrochemical Observation of Single Collision Events: Fullerene Nanoparticles. *ACS Nano* 2014, 8, 7648-7654.
25. Kätelhön, E.; Cheng, W.; Batchelor-McAuley, C.; Tschulik, K.; Compton, R. G. Nanoparticle-Impact Experiments are Highly Sensitive to the Presence of Adsorbed Species on Electrode Surfaces. *ChemElectroChem* 2014, 1, 1057-1062.
26. Sakmann, B.; Neher, E. In *Single-Channel Recording*, 2nd ed.
27. Cheng, W.; Batchelor-McAuley, C.; Compton, R. G. Organic Nanoparticles: Mechanism of Electron Transfer to Indigo Nanoparticles. *ChemElectroChem* 2014, 1, 714-717.
28. Neher, E. Ion Channels for Communication Between and with Cells. *Nobel Lecture, Ion channels for communication between and within cells* 1991.
29. *In some commercial systems other noise sources, for example the analog-to-digital converter, may dominate the noise response.*
30. Schulte, A.; Chow, R. H. A Simple Method for Insulating Carbon-Fiber Microelectrodes Using Anodic Electrophoretic Deposition of Paint. *Analytical Chemistry* 1996, 68, 3054-3058.
31. Lees, J. C.; Ellison, J.; Batchelor-McAuley, C.; Tschulik, K.; Damm, C.; Omanović, D.; Compton, R. G. Nanoparticle Impacts Show High-Ionic-Strength Citrate Avoids Aggregation of Silver Nanoparticles. *ChemPhysChem* 2013, 14, 3895-3897.
32. Bard, A. J.; Faulkner, L. R. *Electrochemical Methods (Wiley, New York, 1980)*.
33. Strein, T. G.; Ewing, A. G. Characterization of Submicron-Sized Carbon Electrodes Insulated with a Phenol-Allylphenol Copolymer. *Analytical Chemistry* 1992, 64, 1368-1373.
34. Wan, Y.; Guo, Z.; Jiang, X.; Fang, K.; Lu, X.; Zhang, Y.; Gu, N. Quasi-Spherical Silver Nanoparticles: Aqueous Synthesis and Size Control by the Seed-Mediated Lee–Meisel Method. *Journal of Colloid and Interface Science* 2013, 394, 263-268.
35. H. S. Toh, K. Jurkschat and R. G. Compton, The Influence of the Capping Agent on the Oxidation of Silver Nanoparticles: Nano-impacts versus Stripping Voltammetry *Chem. – Eur. J.*, 2015, **21**, 2998–3004.
36. Ellison, J.; Tschulik, K.; Stuart, E. J. E.; Jurkschat, K.; Omanović, D.; Uhlemann, M.; Crossley, A.; Compton, R. G. Get More Out of Your Data: A New Approach to Agglomeration and Aggregation Studies Using Nanoparticle Impact Experiments. *ChemistryOpen* 2013, 2, 69-75.
37. Stuart, E. J. E.; Rees, N. V.; Cullen, J. T.; Compton, R. G. Direct Electrochemical Detection and Sizing of Silver Nanoparticles in Seawater Media. *Nanoscale* 2013, 5, 174-177.